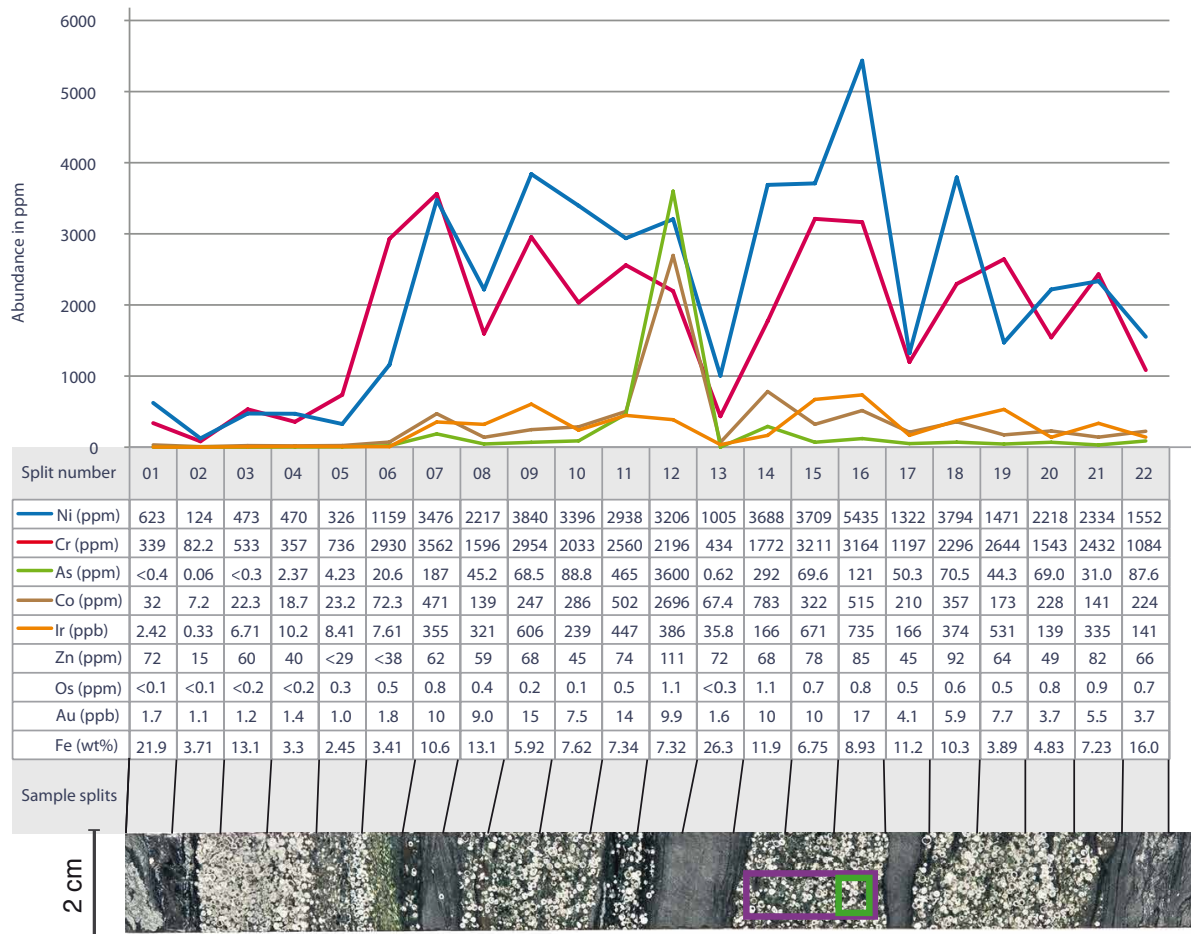


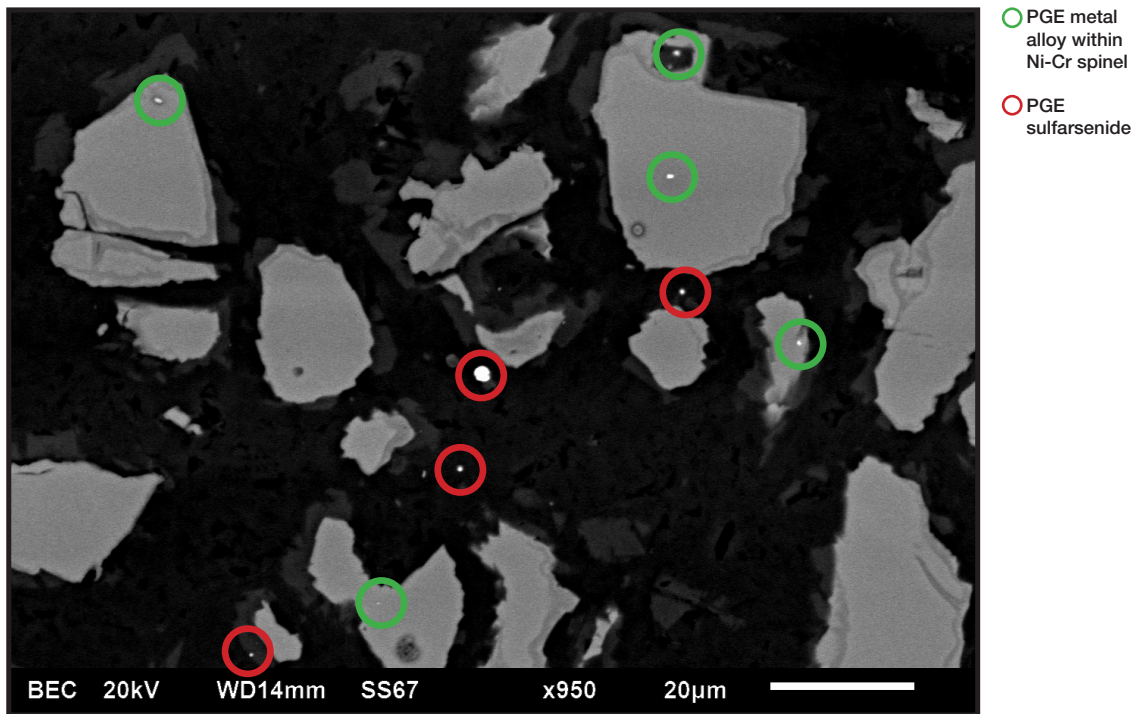
Data repository Mohr-Westheide et al., Discovery of Extraterrestrial Component Carrier Phases in Archean Spherule Layers: Implications for Estimation of Archean bolide sizes

Supplementary Material for Automated feature analysis using a BRUKER QUANTAX EDS system:

The method combines morphological with chemical classification in order to detect and classify minerals (Salge et al., 2013). Grains were detected by grey-scale thresholds in back-scattered electron (BSE) micrographs. Spectra were acquired by point measurements in the center of each grain or by scanning the complete grain area. Minerals were classified based on their composition. An area of $495,613 \mu\text{m}^2$ (Fig. 1, purple rectangle) was analyzed with a pixel resolution of $2 \mu\text{m}$ using an accelerating voltage of 20 kV to detect Ni-Cr-spinel grains with a maximum circle radius $> 6 \mu\text{m}$. For the analysis of PGE phases, the spatial resolution was enhanced to the sub- μm scale by using a low accelerating voltage of 6 kV. Consequently, only low-energy X-ray lines can be evaluated (Figs. 2a,b) which is possible by improved peak deconvolution algorithms using an extended atomic database (Aßmann & Wendt, 2003). A region of $89,746 \mu\text{m}^2$ (Fig. 1, green rectangle) was analyzed with a BSE pixel resolution of 100 nm in order to classify grains with a maximum circle radius $> 250 \text{ nm}$. Regions of interest (Fig. 2c) were further studied by spectrum imaging techniques where a hyperspectral EDS database contains complete spectra for each pixel of the SEM image.



A1 Full data table and plot of INAA results for the 22 sample splits in the ICDP drill core sample BARB 5 (511.29-511.51 m) from the Barite Valley syncline in the BGB. Note sample split 1 is located at the bottom of the sample section, sample split 22 at the top.



A2 Cluster of Ni-Cr-spinel with PGE sulfarsenides in the matrix between individual spinel fragments and PGE metal alloys within Ni-Cr spinel.

A3 Compilation of Ir data from early Archean spherule layers. Evaluating the complete data base of Ir abundances in spherule layer samples in the literature (A3) resulted in: our calculation yielded Ir values from 0.1 to 1518 ppb for S2 (avg. 116 ppb), 0.6 - 2730 ppb for S3 (avg. 164 ppb), 7 - 450 ppb (avg. 128 ppb) for S4, and 0.3 - 735 ppb (avg. 290 ppb) for BARB 5. These Ir concentrations are of equivalent magnitude as those used by Kyte et. al (2003) for estimating Archean bolide/projectile sizes, and still suggest a 30-40% chondrite component, on average, for these layers. However, one has to consider that the Ir concentration in the spherule layer intersections of the BARB 5 core is strongly heterogeneous at the sample scale possibly due to primary heterogeneous fallout from the impact plume,

and not due to dilution by locally derived material as previously reasoned. This is indicated as there is no evidence in the BARB 5 core section for this dilutional process (e.g., addition of clastics). Furthermore, it can not be excluded either that alteration and metamorphic overprint may have affected the primary PGE abundances of spherule deposits.

TABLE A4. ELECTRON MICROPROBE ANALYSES OF NI-RICH CORES (A) AND ZN-ENRICHED RIMS (B) OF NI-CR SPINELS FROM SPHERULE LAYERS FROM DRILL CORE BARB 5.

Major elements (wt %)	ON TOP OF SL 1' ($n_a = 17$, $n_b = 5$)				SL 2' ($n_a = 134$, $n_b = 6$)				SL 3' ($n_a = 107$, $n_b = 4$)				SL 4' ($n_a = 101$, $n_b = 4$)			
	Range		Average		Range		Average		Range		Average		Range		Average	
			SD*	SD*			SD*	SD*			SD*	SD*			SD*	SD*
A	SiO ₂	0.74	-	0.92	0.83	0.05	0.31	-	1.45	0.72	0.25	0.37	-	1.46	0.76	0.22
	Al ₂ O ₃	0.63	-	0.76	0.70	0.04	0.08	-	2.28	0.31	-	10.68	-	2.76	0.22	0.12
	TiO ₂	0.07	-	0.16	0.11	0.03	0.01	-	0.68	0.23	0.17	0.03	-	0.92	0.26	0.22
	Cr ₂ O ₃	38.09	-	43.49	40.08	1.57	34.01	-	53.43	41.09	4.80	0.02	-	56.95	4.93	32.52
	MnO	0.08	-	0.11	0.10	0.01	0.06	-	0.14	0.09	0.02	0.06	-	0.13	0.08	0.01
	FeO	0.09	-	0.20	0.21	0.32	0.08	-	4.90	1.57	1.12	0.09	-	7.22	1.51	0.09
	CoO	40.59	-	46.75	43.43	1.86	26.41	-	46.47	35.67	4.21	26.43	-	46.23	3.76	27.01
	NiO	0.06	-	0.41	0.25	0.13	0.06	-	0.53	0.31	0.10	0.01	-	0.71	0.33	0.14
	ZnO	6.94	-	11.01	9.18	1.24	7.34	-	19.42	14.21	2.95	18.71	-	12.44	3.02	9.83
B	V ₂ O ₃	0.00	-	1.31	0.44	0.42	0.00	-	1.27	0.12	0.26	0.00	-	2.42	0.22	0.43
	SiO ₂	0.65	-	0.72	0.69	0.02	0.39	-	2.45	1.27	0.51	0.12	-	2.47	0.49	0.58
	Al ₂ O ₃	0.99	-	1.41	1.21	0.18	0.70	-	1.42	1.07	0.29	0.65	-	1.48	1.08	0.35
	TiO ₂	0.13	-	1.08	0.93	0.13	0.99	-	3.93	1.74	1.11	0.47	-	5.94	2.87	0.48
	Cr ₂ O ₃	38.60	-	40.41	39.59	0.83	36.17	-	40.30	38.20	1.62	33.66	-	44.96	39.36	4.85
	MnO	0.08	-	0.10	0.09	0.03	0.07	-	0.09	0.13	0.08	0.06	-	0.10	0.07	0.00
	FeO	42.36	-	47.11	45.53	1.86	44.85	-	46.67	45.89	0.67	41.05	-	47.36	3.10	46.07
	CoO	0.00	-	0.12	0.03	0.05	0.00	-	0.04	0.02	0.02	0.00	-	0.12	0.03	0.01
	NiO	4.20	-	7.48	5.28	1.37	2.70	-	6.20	5.07	1.44	0.71	-	5.22	2.81	3.19
	ZnO	1.01	-	3.19	1.86	0.85	0.84	-	3.95	1.93	1.18	1.74	-	6.29	2.64	3.81
	V ₂ O ₃	0.66	-	0.74	0.70	0.03	0.93	-	2.05	1.57	0.48	0.81	-	1.59	1.28	0.34

*SD = Standard deviation

**SL = Spherule layer

TABLE A3. SUMMARY OF IR CONCENTRATION SYSTEMATICS (DATA IN PPB) IN SPHERULE LAYERS OF THE BOB.

Kyte et al., 2003	Average	6 (n = 1)	SL 1' (n = 56')				SL 2' (n = 54')				SL 3' (n = 22')				SL 4' (n = 34')				Host rock (n = 6')				BARB 5				
			SL 1' (n = 56')	Host rock (n = 54')	S2	SL 1' (n = 78')	Host rock (n = 22')	S3	SL 1' (n = 34')	Host rock (n = 6')	S4	SL 1' (n = 34')	Host rock (n = 6')	S5	SL 1' (n = 22')	Host rock (n = 6')	S6	SL 1' (n = 22')	Host rock (n = 6')	S7	SL 1' (n = 19')	Host rock (n = 6')	S8	SL 1' (n = 22')			
			0.10	0.07	5.87	0.60	0.12	3.40	3.40	0.77	0.62	4.90	119	0.31	0.12	0.07	0.01	0.06	0.09	0.01	0.07	0.01	0.06	0.01	0.07		
			1518	277	1.25	116	1.14	164	0.60	0.60	1.04	1.25	240	128	0.20	0.13	0.00	0.00	0.00	0.00	0.00	0.00	0.00	0.00	0.00	0.00	
			116	6	-	519	-	519	0.60 (n = 1)	0.60 (n = 1)	449 (n = 3)	449 (n = 3)	197 (n = 2)	197 (n = 2)	0.13	0.13	0.13	0.13	0.13	0.13	0.13	0.13	0.13	0.13	0.13	0.13	0.13

*SL = Spherule layer

**SL = SL without split Nos. 1, 13, 22 (mixed shale/SL material)

¹Lowe et al., 1989; Koebel et al., 1995; Reimold et al., 2000; Lowe et al., 2003²Lowe et al., 1989; Koebel et al., 1993; Reimold et al., 2000; Lowe et al., 2003³Lowe et al., 1989; Koebel et al., 1995; Reimold et al., 1995; Hofmann et al., 2006⁴Lowe et al., 1989; Koebel et al., 1993⁵Kyte et al., 1992; Lowe et al., 2003⁶Kyte et al., 1992

REFERENCES CITED

- Aßmann, A., and Wendt, M., 2003, The identification of soft X-ray lines: *Spectrochimica Acta Part B*, v. 58, p. 711-716.
- Hofmann, A., Reimold, W.U., and Koeberl, C., 2006, Archean spherule layers in the Barberton greenstone belt, South Africa: a discussion of problems related to the impact interpretation, *in*, Reimold, W.U., Gibson, R.L. eds., Processes of the Early Earth. Boulder: Geological Society of America Special Paper 405, p. 33–56.
- Koeberl, C., Reimold, W.U., and Boer, R.H., 1993, Geochemistry and mineralogy of Early Archean spherule beds, Barberton Mountain Land, South Africa: evidence for origin by impact doubtful: *Earth and Planetary Science Letters*, v. 119, p. 441–452, doi: 10.1016/0012-821X(93)90152-Y.
- Koeberl, C., and Reimold, W.U., 1995, Early Archean spherule beds in the Barberton Mountain Land, South Africa: no evidence for impact origin: *Precambrian Research*, v. 74, p. 1-33, doi: 10.1016/0301-9268(94)00099-D.
- Kyte, F.T., Zhou, L., and Lowe, D.R., 1992, Noble metal abundances in an Early Archean impact deposit: *Geochimica et Cosmochimica Acta*, v. 56, 1365–1372, doi: 10.1016/0016-7037(92)90067-S.
- Kyte, F.T., Shukolyukov, A., Lugmair, G.W., Lowe, D.R., and Byerly, G.R., 2003, Early Archean spherule beds: chromium isotopes confirm origin through multiple impacts of projectiles of carbonaceous chondrite type. *Geology*, v. 31, p. 283–286, doi: 10.1130/0091-7613(2003)031<0283:EASBCI>2.0.CO;2.
- Reimold, W.U., Koeberl, C., Johnson, S., and McDonald, I., 2000, Early Archean Spherule Beds in the Barberton Mountain Land, South Africa: Impact or Terrestrial Origin, *in* Gilmour, I., and Koeberl, C., eds., Impact and the Early Earth: Berlin-Heidelberg, Springer-Verlag, v. 91, p. 117-180.

Lowe, D.R., Byerly, G.Y., Asaro, F., and Kyte, F.T., 1989, Geological and Geochemical Record of 3400-Million-Year-Old Terrestrial Meteorite Impacts: Science, v. 245, p. 959-961.

Lowe, D.R., Byerly, G.Y., Kyte, F.T., Shukolyukov, A., Asaro, F., and Krull, A., 2003, Spherule Beds 3.47–3.24 Billion Years Old in the Barberton Greenstone Belt, South Africa: A Record of Large Meteorite Impacts and Their Influence on Early Crustal and Biological Evolution: Astrobiology, v. 3, p. 7-48, doi: 10.1089/153110703321632408.

Salge, T., Neumann, R., Andersson, C., Patzschke, M., 2013, Advanced mineral classification using feature analysis and spectrum imaging with EDS, *in* Proceedings: International Mining Congress and Exhibition, 23rd, Turkey, UCTEA Chamber of Mining Engineers of Turkey, p. 357-367.